



Process-based eco-hydrological modeling in an Eastern Himalayan watershed using RHESSys

Pooja Mishra¹ · Ngahorza Chiphang¹ · A. Bandyopadhyay¹ · A. Bhadra¹

Received: 7 June 2020 / Accepted: 27 November 2020 / Published online: 11 January 2021
© The Author(s), under exclusive licence to Springer Nature Switzerland AG part of Springer Nature 2021

Abstract

Hydro-ecological models are important tools used to estimate streamflow from mountainous watersheds as driven by precipitation and snowmelt under the influence of different spatially variable hydro-ecological response variables. These models enable us to gain insight into hydrological and ecological processes occurring in the watershed. In the present study, a hydro-ecological model, Regional Hydro-Ecological Simulation System (RHESSys) was set up for a small representative watershed in Eastern Himalayan region of Arunachal Pradesh to investigate spatial variation in saturation deficit during snow depletion period. RHESSys model is capable of estimating variations in evaporation, transpiration, streamflow, overland flow, saturation deficit, etc. from the landscape. Studies related to hydrological and ecological sustainability of the Eastern Himalayan Rivers are limited, although a major part of the region is covered with evergreen forests, where ecological parameters may have a great impact on watershed hydrology. Nuranang watershed, which is located in Tawang district of Arunachal Pradesh, India, was selected as the study area. The hydro-meteorological data from 2004 to 2008 were collected from Central Water Commission (CWC). Digital Elevation Model (DEM) with 30 m spatial resolution was downloaded from NASA website. Calibration of the RHESSys model was performed for the depletion period of 2004 (13th April–21st August) and 2005 (17th April–4th September) and the model was validated for the years 2008 (17th April–20th September) and 2009 (13th April–23rd September) using observed streamflow at the watershed outlet. Comparison plot of the actual and log values of observed and simulated daily discharges showed that the model captured the variations in total observed discharge and subsurface flows reasonably well for both the calibration and validation years. Daily time-series outputs of various hydrological variables, i.e., subsurface flow, overland flow, streamflow, saturation deficit, and percentage saturated area, were obtained for both calibration and validation simulation. For simulation years, overland flow dominated stream discharge in all the months, and contributed around 60% of the total streamflow, whereas subsurface flow contributed around 40% in all the months. Comparatively, saturation deficit was more in the month of April due to less precipitation and it was reduced in the month of May because of pre-monsoon rainfall. It increased again in the month of June as the precipitation in the month was less compared to May. Then, it decreased again in the subsequent months of July and August due to high rainfall during the monsoon season and increased in the month of September. Average saturation deficit was estimated to be 389.69 mm and average percentage saturated area was estimated as 9.52%. The number of saturated pixels was found to be minimum in the month of April, while a maximum number of saturated pixels were observed in the month of August indicating the existence of inverse relationship between precipitation and saturation deficit for the study area.

Keywords Hydro-ecological model · Rhesys · Spatially variable terrain · Eastern himalayan region · Saturation deficit

Introduction

Water resource management and water availability are important factors of the environment, ecosystem, and economy of a particular region. The climate system and the river regimes of any particular region are highly variable on both the inter-annual and intra-annual timescales. Hydrological modeling is an effective technique, which is increasingly

✉ A. Bandyopadhyay
arnabbandy@yahoo.co.in

¹ Department of Agricultural Engineering, North Eastern Regional Institute of Science and Technology, Nirjuli, Itanagar, Arunachal Pradesh 791109, India

used to manage and develop the water resources. These models are useful in understanding the processes governing the flow of water and river characteristics in mountains, which are extremely important for suitable water resource management in the downstream areas. Hydrological models also allow estimating the response of hydro-ecological variables to changes in climatic conditions. Hydro-ecological model can be used to estimate streamflow from a mountainous basin, caused by precipitation and snowmelt under different spatially variable hydro-ecological response variables. Watershed routing and vegetation are the important factors which mostly control the hydrological response of a watershed. Routing affects the soil moisture distribution and hence the peak runoff timing at the watershed outlet (Praveen et al. 2016). Vegetation cover influences the overland flow by intercepting precipitation which evaporates back to the atmosphere and influencing the evapotranspiration rate. Distributed watershed-scale models have been used increasingly to obtain the streamflow from the watershed and for the assessment of climate and land-use change impacts.

Numerous hydrologic models have been applied in several agro-climatic regions for the estimation of streamflow and obtaining the impact of climate change on streamflow. Mishra and Lihare (2016) simulated monthly streamflow for some selected basins in the Indian subcontinent using the SWAT model and reported an acceptable performance by the model. Chaemiso et al. 2016 used the SWAT model and evaluated the runoff from Ilala watershed, Northern Ethiopia under RCP 4.5 and 8.5 scenarios. They reported an increase in the minimum and maximum temperatures for the future years, while rainfall did not show any significant increasing or decreasing trend for the study area. The rainfall–runoff relationship was strongly correlated with $R^2 = 0.97$. Aawar and Khare, 2020 applied the SWAT model to assess the climate change impact on streamflow in Kabul River basin, Afghanistan. Results showed that the streamflow in the region was directly influenced by change in temperature and precipitation. Apart from these, many other studies have successfully applied the SWAT model for streamflow simulations (Chaemiso et al. 2016; Paul and Negahban-Azar 2018; Khatun et al. 2018; Boufala et al. 2019; Hosseini and Khaleghi 2020; Patil and Nataraja 2020). Other than SWAT, VIC model (Variable Infiltration Capacity) (Shah and Mishra 2016; Chawla and Mujumdar 2015), and HEC-HMS model (Hydrologic Engineering Centre-Hydrological Modeling System) (Cahyono and Adidarma 2019; Natrajan and Radhakrishnan 2019; Meresa 2019; Mandal and Chakraborty 2016) have also been applied in many watersheds.

Regional Hydro-Ecological Simulation System (RHESSys) is a hydro-ecologic model which has continuously been used for obtaining the temporal and spatial variation of soil moisture, saturation deficit, and the leaf area index of canopy at the watershed scale (Band et al. 2001). It

is a spatially distributed model which works on daily time step and solves coupled soil/canopy water, carbon, and nutrient budgets within a watershed. The model uses streamflow data from a watershed outlet to validate the mass balance of water cycle, which is not affected by topographic and climatic conditions of the watershed (Hwang et al. 2008). RHESSys has been and continues to be successfully applied and validated in numerous forested catchments. The model has been applied to the watershed area ranging from as small as 0.1 km² (Tsamir et al. 2019) to 60,000 km² (Baron et al. 1998). It was observed that RHESSys is more suitable for eco-hydrological modeling of small catchments (Gorelick et al. 2020). The ability of the model to predict streamflow, nitrate export, net photosynthesis, and sensitivity of streamflow to changes in land use/land cover of the study region has been documented in many studies. In the first version of RHESSys, the biogeochemical model BIOMEGC was coupled with the distributed hydrological model TOPMODEL (Band et al. 1993). The model was further developed (Hartman et al. 1999; Tague and Band, 2001) and successfully evaluated. Band et al. (2001) evaluated and predicted the distribution of water, carbon, and nitrogen cycling by applying RHESSys model. The outputs from the model were calibrated and validated with measured streamflow data. Tague and Band (2004) evaluated the performance of RHESSys by comparing the model outputs to that of the MIKESHE model which is similar to RHESSys in terms of complexity. Sanford et al. (2007) used RHESSys to characterize the natural flow regime of first-to-fifth-order basins using the range of variability approach. Kim et al. (2007) applied RHESSys to a catchment for optimum model parameterization and evaluation of eco-hydrological processes variation.

Mohammed and Tarboton (2014) used RHESSys to examine the sensitivity of streamflow to the change in land cover in a highland catchment. Morán-Tejeda et al. (2015) compared the performance of RHESSys and SWAT in the same watershed with the same inputs. They found that RHESSys was found more sensitive to vegetation change, since RHESSys estimates evapotranspiration in process-based way, and therefore, RHESSys model is more suitable for watershed covered having dominant with forest cover. Mengistu et al. (2016) investigated eight different patch configurations of a sub-catchment to analyze the effect of patch characterization/formation in streamflow simulation, using the RHESSys model. Shin et al. (2019a, b) examined the effects of future climate changes on watershed hydro-ecology, including runoff, evapotranspiration, soil moisture content, gross primary production, and photosynthetic productivity, by applying the RHESSys model to the Seolmacheon catchment (8.5 km²).

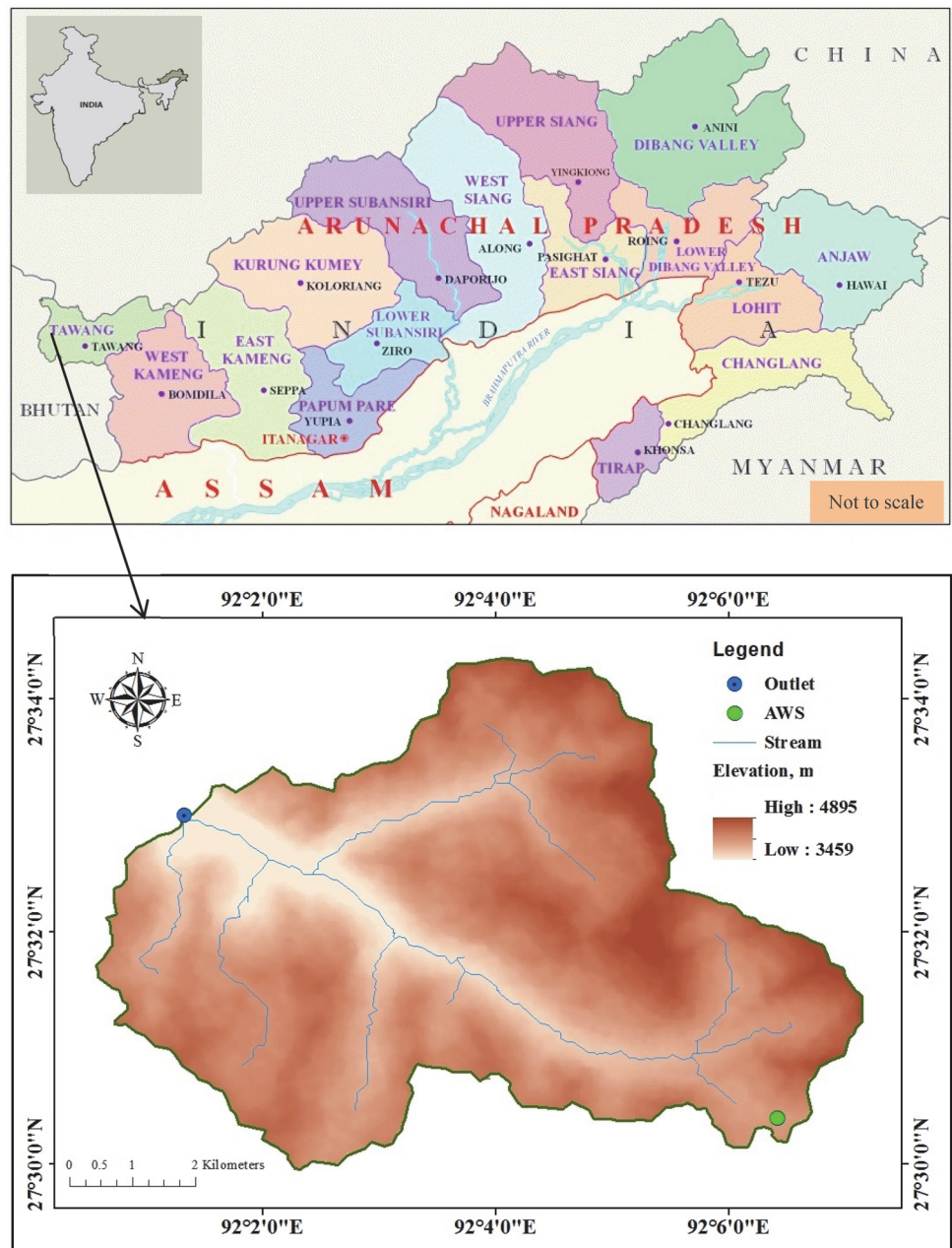
Although a major part of the Eastern Himalayan region is covered with lush evergreen forest and higher elevation

ranges are mostly covered with seasonal snow, studies related to hydrological and ecological sustainability of the Eastern Himalayan rivers are limited. Hydro-ecological modeling studies on the forested catchment of Arunachal Pradesh have not been reported so far in the literature. These regions are physio-graphically diverse and ecologically rich in natural and crop-related biodiversity. In the present study, the RHESSys model was applied for the spatial assessment of the saturation deficit during snow depletion period in an Eastern Himalayan watershed of Arunachal Pradesh.

Study area and data acquisition

Nuranang watershed (Fig. 1), draining an area of 52.37 km², located at Tawang district of Arunachal Pradesh, India, was selected as the study area. The area lies between North latitudes from 27° 29' 57.37" to 27° 34' 21.15" and East longitudes from 92° 00' 33.98" to 92° 07' 08.93" with an elevation ranging from 3459 to 4895 m above mean sea level (MSL). Nuranang River, a tributary of Tawang River, originates from Sela Lake and joins Tawang River as Nuranang falls at Jang. The altitude of the Sela Lake is 4,211 m above MSL and it lies at 27° 30' 09" N and 92° 06' 17" E. The

Fig. 1 Nuranang watershed, Arunachal Pradesh, India



discharge site of Central Water Commission (CWC) at RA-III, Jang was selected as the outlet point at 27° 33' 00" N and 92° 01' 19" E, with an elevation of 3,459 m above MSL. Monsoon season starts from May and last till September having average annual precipitation of 1139 mm. The entire watershed receives snowfall in the winter season (October–March). Depletion period starts from mid-February and lasts till early June with snow accumulation and depletion periods varying a little year-to-year. Soils in the region are rich in organic content and are highly acidic in nature.

The meteorological and hydrological data of Nuranang watershed from 2004 to 2009; measured at CWC discharge site at RA-III, Jang, were collected from CWC office, Itanagar, Arunachal Pradesh. Observed maximum and minimum temperatures from 2016 to 2017 were taken from the AWS installed at 27° 30' 09" N latitude and 92° 06' 17" E longitude and at an altitude of 4211 m above MSL. As CWC discontinued its discharge site at RA-III, Jang (the selected outlet point of Nuranang watershed for this study) in 2011, a radar-type automated gauge recorder (DWLR) was installed at the outlet of Nuranang watershed in the month of April 2015. Later, in September 2016, additional AT/RH (air temperature and relative humidity) sensors were also added with the DWLR for estimation of near-surface temperature lapse rate. Maximum and minimum air temperatures determined from the hourly temperature records of AWS and DWLR were used for validating the near-surface temperature lapse rate of the watershed. The Digital Elevation Model (DEM) with 30 m spatial resolution was downloaded for the study area (3459–4892 m) from the website of National Aeronautics and Space Administration (NASA) (<http://reverb.echo.nasa.gov/reverb/>). Soil map for the state was taken from the State Land Use Board (SLUB), Govt. of Arunachal Pradesh (Srivastava 2000). The Land-Use/Land-Cover (LULC) map for the state of Arunachal Pradesh was purchased from the State Remote Sensing Application Centre (SRSAC), Department of Science and Technology, Govt. of Arunachal Pradesh. Twenty-seven soil samples from the top layer (0–30 cm) were collected from different elevation zones of Nuranang watershed. Elevation range of the sampling points varied from 3481 to 4215 m above MSL.

Methodology

Pre-processing and analysis of data

The ASTER DEM downloaded in Geographic Coordinate System (GCS) was projected to the Universal Transverse Mercator (UTM) Projected Coordinate System (PCS) and exported to ASCII (.asc) format using ArcMap 10.0, which was then imported to Geographic Resources Analysis Support System Geographic Information System (GRASS-GIS).

Nuranang watershed was delineated using DEM considering CWC discharge site as the outlet point. LULC shapefile for the entire Arunachal Pradesh obtained from the SRSAC was clipped for the study area. The shapefile was converted to raster format with the same spatial resolution as the DEM. Raster map was converted to ASCII (.asc) format using ArcMap 10.0 and was directly imported into GRASS for analysis. Eight LULC classes were found in the study region, namely, Alpine Grass, Barren Rocky/Stony Waste/Sheet Rock Area, Degraded/Scrub Forest, Evergreen/Semi-Evergreen Forests (Dense), Lake/Pond, Land with Scrub, Snow-Covered/Glaciated Area, and Village. The soil map for the study area collected from SLUB was scanned, geo-referenced, and digitized in ERDAS IMAGINE 2014. The digitized shapefile of soil map was then converted to raster and exported to ASCII format with the same spatial resolution as DEM, which was then imported in GRASS for analysis. Four types of soil were found in the study area, namely, Loamy Skeletal Typic Udorthents, Loamy Skeletal Entic Haplumbrepts, Loamy Skeletal Lithic Udorthents, and Sandy Skeletal Typic Udorthents.

Determination of temperature lapse rate

Temperature lapse is defined as the rate of decrease of atmospheric temperature with increase in altitude vertically above a particular location. The near-surface air temperature has a great impact on water cycle of the region as it governs complete environmental processes (Prihodko and Goward 1997; Bolstad et al. 1998). In RHESys, temperature lapse rate is required as input in the zone default file of every zone for interpolating temperature for each pixel from the point time-series input of temperature. Since measured time-series data for climatic variables are available only at the outlet of the watershed, the entire watershed was considered as only one zone.

Bandyopadhyay et al. (2014) estimated the mean temperature lapse rate in Arunachal Pradesh. Hourly data of meteorological parameters, and maximum and minimum temperatures from 18 stations of Arunachal Pradesh for the period of 5 years (2004–2008) were analyzed. Lapse rate varied within 0.32–0.56, 0.44–0.54, and 0.36–0.52 °C/100 m for maximum, minimum, and average temperatures, respectively, with an average value of around 0.5 °C/100 m. This value of lapse rate was estimated for the whole of Arunachal Pradesh, as such validation of lapse rate for the Nuranang watershed was necessary. The value was validated with the temperature lapse for the watershed calculated using the temperatures measured at the Sela Top (AWS site) at 4211 m elevation and at the outlet of the watershed (DWLR site) at 3459 m elevation. Temperature lapse rate of the watershed was estimated to be around 0.48 °C/100 m during 2016–2017, which matched well with the temperature lapse

rate found for Arunachal Himalaya. This value of lapse rate was used in the zone default file for RHESSys model setup.

Analysis of soil properties over spatially variable terrain

Various soil physical and chemical properties are required in RHESSys for preparation of the soil default file for each soil type as these properties affect the watershed yield potential. The process of transformation of precipitation to stream outflow is a very complex process, which is mainly governed by soil properties. Soil properties influence the infiltration rate, drainage, and erosion, which in turn influence the runoff from the watershed. Overland flow occurs only when rainfall rate over a region exceeds the infiltration rate of the soil (Schwab et al. 1993; Le Bissonnais et al. 2005). Therefore, various physical and chemical properties of the collected soil samples, such as textural class, porosity, pH, etc., were determined for further use.

The soil bulk density (BD) of the samples ranged from 0.70 to 1.20 (g cm^{-3}). The BD of the collected soil samples was lower than the normal range (1.1–1.6 g cm^{-3}) because of the presence of high organic matter content. Organic soils have high fiber contents, which create a more open structure resulting in more voids, leading to low bulk density. Moisture content ranged from 5 to 218% for the collected soil samples from different elevation zones of the watershed. The specific gravity of the samples ranged from 1.35 for soils at higher elevations to 2.78 for soils at lower elevation.

Sand and silt percentages increased with altitude, whereas clay percentages decreased significantly with the altitude of the sampling points. Sand % of the watershed soil was found to vary from 80.17 to 95.20%, whereas Silt % varied from 14.93 to 15.87%. Clay % was found varying from 0 to 9.33%. Hence, it can be inferred from the findings that the soils of this region are dominated by sand.

The void ratio ranged from 1.73 to 7.10 for the soil samples collected from different elevation zones of the watershed. The porosity of the collected soil samples ranged from 0.63 to 0.88 which showed that the soils in the watershed are highly porous. All the soil samples collected were observed to be acidic. The pH values ranged from 3.354 to 6.615 with an average of 5.08.

Soil properties obtained at various locations for particular soil types were averaged to obtain a single value of each soil property and these values were used as input in the soil default file of the RHESSys setup, along with the spatial map of soil type. Soil physio-chemical properties that are required in the soil default file include soil pH, porosity, sand %, silt %, and clay %. The values of soil properties remain constant throughout the model run for each soil type.

The change in altitudinal gradients influences soil properties by controlling soil–water balance, soil erosion, etc.

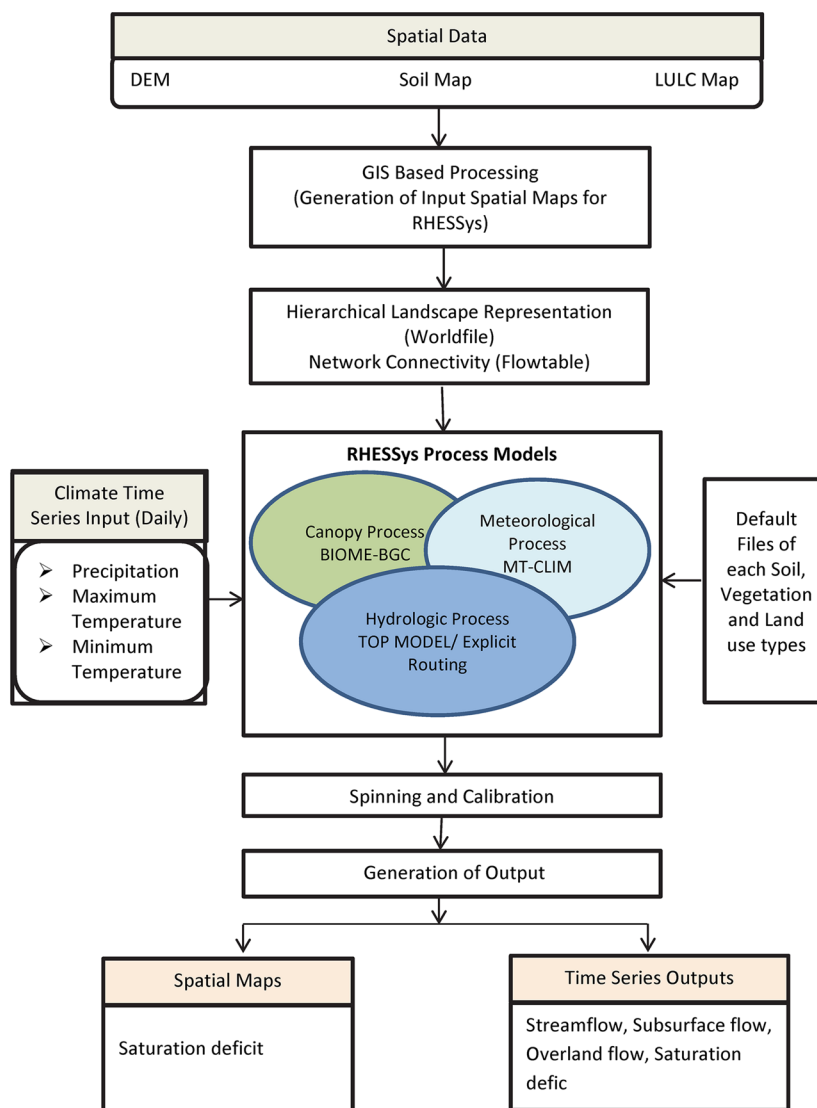
Pearson correlation coefficient was determined for the analysis of correlation of different physio-chemical properties of soil with altitude using SPSS statistical software for Windows. pH was found to be significantly negatively correlated with the elevation with a Pearson correlation coefficient of -0.539 at a significance level of 0.01. Clay % and specific gravity decreased significantly with a Pearson correlation coefficient of -0.338 and -0.64 at 0.05 and 0.01 significance levels, respectively. Moisture content, void ratio, and porosity were found positively correlated with a Pearson correlation coefficient of 0.634, 0.464, and 0.444 at a significance level of 0.01, 0.05, and 0.05, respectively. Sand and Silt percentages increased with the increase in elevation and bulk density decreased with elevation but were very poorly correlated.

RHESSys

RHESSys (Fig. 2) is a GIS-based, hydro-ecological modeling framework that combines both a set of physically based process models and a methodology for partitioning the landscape and parameterizing the model. The process models simulate runoff over a spatially variable terrain at small-to-medium scales. RHESSys allows analyzing the hydro-ecological interactions at several spatial scales from a hill slope to whole basins (Band et al. 1993). The model computes different hydrological, climatic, and vegetation processes at related patch scales and allows upscaling them to the landscape. RHESSys couples an ecosystem carbon-cycling model with a spatially distributed hydrology model. RHESSys considers the spatial variances of micro-climate and soil water in simulating water and carbon dynamics of forest ecosystem. Model inputs consist of climate time-series characterizing the vertical fluxes of water and energy, and GIS layers characterizing the catchment physical properties that determine catchment processing of mass and energy, including topography, soils, vegetation, and impervious cover. RHESSys can simulate both hydrologic and vegetation processes within a spatial context. In this study, RHESSys daily output of saturation deficit, saturated area percentage, base flow, saturation overland flow, and total stream outflow were analyzed.

The three process-based models in RHESSys comprise a climate model, MTN-Clim that uses the user-supplied climate input to extrapolate other input climate variables. RHESSys includes two distributed hydrological models, TOPMODEL to model soil moisture distribution and runoff generation, and an explicit routing model DHSVM (Distributed Hydrology Soil Vegetation Model) to model saturated surface interface and overland flow.

Fig. 2 Input and output of RHESSys model under present study



Theoretical consideration in RHESSys

RHESSys uses a physically based watershed model, TOPMODEL (Beven and Kirkby 1979) for generation of total streamflow from patches and at the outlet of the basin. The model uses the variable-source-area concept of streamflow generation. Model predictions include estimations of streamflow, overland, subsurface flow, and an estimate of the spatial pattern of the depth to the water table in the watershed. TOPMODEL relationships are based on the assumption that saturated hydraulic conductivity varies exponentially with depth, that water table gradients can be approximated by local topographic slope, and that steady-state flux is achieved within the modeling time step. A full description of processes used in streamflow generation in RHESSys is given in Wolock (1993) and Tague and Band (2004). Infiltration at each time step is estimated following

Phillip's infiltration equation (Phillip 1957), potential capillary rise from the unsaturated zone is calculated based on the approach used by Eagleson (1978), and both evaporation and transpiration rates are computed using standard Penman–Monteith (Monteith 1965) equation.

The explicit routing model in RHESSys is based on DHSVM routing approach that has been modified to account for non-grid-based patches and non-exponential transmissivity profiles. DHSVM assumes that hydraulic gradients follow surface topography. Flow topology is generated by a GIS-based preprocessing routine, CREATE_FLOWPATHS. Multiple flow directions, from any given patch, are permitted.

Surface flow (i.e., saturation overland flow or Hortonian overland flow) produced is routed following the same patch topology used from routing saturated subsurface throughflow. All surface flow produced by a patch is assumed to

exit from the patch within a single time step. If the receiving patch is not saturated, surface flow is allowed to infiltrate and is added to unsaturated soil moisture storage. Patch routing is sequenced to start from the uppermost patches in the watershed.

Preparation of input datasets for RHESSys

Various spatial data/maps are required in RHESSys to form a complete landscape representation and to establish connectivity between spatial units in the basin. Spatial maps required for the analysis were prepared from DEM and other spatial maps (LULC and soil maps). The maps derived using DEM were basin, slope, aspect, hillslope, patch, saturated soil hydraulic conductivity at the surface (K_{sat_0}), decay of hydraulic conductivity with depth (m), stream network, and roads. GRASS GIS was used to process and store the set of spatial data layers/maps required. Vegetation and soil maps were directly imported in GRASS. In RHESSys, the landscape is divided into four different land uses, namely, agricultural, urban, undeveloped, and residential. As there was no agricultural, urban, or residential area in the watershed, the whole basin was classified as a single undeveloped land-use type and no land-use map was prepared.

Climate input and processing in RHESSys are done at the zone level. In the present study, only essential climate inputs, i.e., maximum temperature (°C), minimum temperature (°C), and precipitation (m) measured at the outlet of the watershed were used to run the model. For a given time-step, each climate variable associated with a base station was contained in a separate file. Climate data obtained from CWC were used as climate inputs.

In addition to the spatial maps and climate time-series input, RHESSys requires some other variables. The values of these variables are stored in the default files and are kept constant through the model run. Different default files required in RHESSys are Basin Default File, Hillslope Default File, Zone Default File, Soil Default File, Land Use Default File, and Stratum/Vegetation Default File. The basin and hillslope default file structures contain only default file identifier, and the zone default file contains atmospheric parameters associated with zone objects. Temperature lapse rate estimated for Nuranang watershed was used in the zone default file. A single-zone default file was made as there was

only one zone in the study area. Soil default files describe characteristics of particular soil types. Various physical and chemical properties of the soil samples collected from different elevations of the watershed were used for the preparation of the soil default file. Since the whole of the watershed was taken as undeveloped, only one default file was prepared for undeveloped land-use type. Default file for each of the four vegetation types was directly taken from the RHESSys library.

Stabilization of soil and plant carbon and nitrogen under spinning-up

In RHESSys simulations, spinning-up is done to allow carbon and nitrogen stores to stabilize. The time required for the model to reach equilibrium depends on the characteristics of the landscape (i.e., type of climate, vegetation, and soil). To determine the stability of the model, RHESSys outputs for plant and soil N and C from the spin-up simulations were evaluated. Carbon and nitrogen cycling in RHESSys is modified from BIOME-BGC (Thornton 1998). The output variables, i.e., plantc, plantn, soilc, and soiln, were examined after 75 years and 225 years of processing, to see how these variables were changing and moving toward stabilization. The model was considered stable when the plant and soil C and N variables did not trend up or down.

Model calibration and validation

Model calibration consisted of modifying values of model parameters in an attempt to match field conditions within some acceptable criteria. Four independent parameters of RHESSys are the decay of hydraulic conductivity with depth (m), saturated soil hydraulic conductivity at surface (K), and two groundwater parameters which control the proportion of infiltrated water that bypasses soil (via macropores and fractures) to a deeper groundwater table (gw1), and the rate of lateral flow from a hillslope scale groundwater table (modeled as a linear reservoir) to the stream channel (gw2). These calibrated values are multipliers, which are multiplied with the original value provided in the input parameters file. Five hundred sets of random values for calibrated parameters within their typical ranges (Table 1) were generated using R programming language to obtain an adequate sample across

Table 1 RHESSys calibration parameters for years 2004 and 2005

Sl. No	Calibration parameter	Description	Calibrated value		Average
			2004	2005	
1	<i>m</i>	Decay of hydraulic conductivity with depth	0.1944	0.1007	0.1475
2	<i>K</i>	Saturated soil hydraulic conductivity at surface	46.3015	34.3757	40.3386
3	<i>gw1</i>	Groundwater parameter	0.2161	0.2620	0.2391
4	<i>gw2</i>	Groundwater parameter	0.2292	0.1675	0.1983

the full range of each parameter. The model was calibrated using the observed streamflow from the watershed at the outlet for the years 2004 and 2005. The best set of calibration parameters were identified by comparing simulated and observed streamflow. Four dimensionless statistical performance criteria, viz., Modeling Efficiency (ME), Coefficient of Residual Mass (CRM), Coefficient of Determination (R^2), and Standard Error of Estimate (SEE), were used to identify the best set of calibration parameters. Reasonable values for the calibrated parameters (m , K , $gw1$, and $gw2$) were obtained by measuring the correspondence of modeled streamflow to the observed streamflow for goodness of fit.

The calibrated model parameters obtained for the years 2004 and 2005 were averaged to obtain calibration parameter for the watershed. The calibration parameter obtained

was validated using the model-simulated streamflow for years 2008 and 2009. Daily time-series outputs of various hydrological variables, i.e., subsurface flow, overland flow, streamflow, saturation deficit, and percentage saturated area, were obtained for both calibration and validation simulations using the best set of calibration parameters. From the daily time-series outputs, patch outputs of saturation deficit were generated to visualize the output spatially. RHESSys output variables can be viewed spatially in GRASS GIS program by replacing the raster map ID numbers with values for a particular output variable. The variable to be viewed was extracted from the patch.daily RHESSys output file using Command line language AWK.

Results and discussion

Stabilization of soil and plant carbon and nitrogen under spinning-up

Soil and plant carbon (C) and nitrogen (N) were stabilized for both the calibration (2004 and 2005) and validation (2008 and 2009) years. The RHESSys model was run for 225 years of spin-up. RHESSys outputs of soil and plant C and N were taken from the output file. Plant and soil Nitrogen and Carbon for each run is calculated using BIOME-BGC (Thornton

Table 2 Model performance for calibration years

SI No	Performance indicator	Actual streamflow		Log of streamflow	
		2004	2005	2004	2005
1	ME	0.754	0.816	0.589	0.786
2	CRM	0.023	0.006	0.041	0.053
3	R^2	0.782	0.873	0.718	0.108
4	SEE	1.187	0.966	0.122	0.864

Fig. 3 Daily time-series plots for actual and log values of the observed and simulated streamflows for calibration year 2004

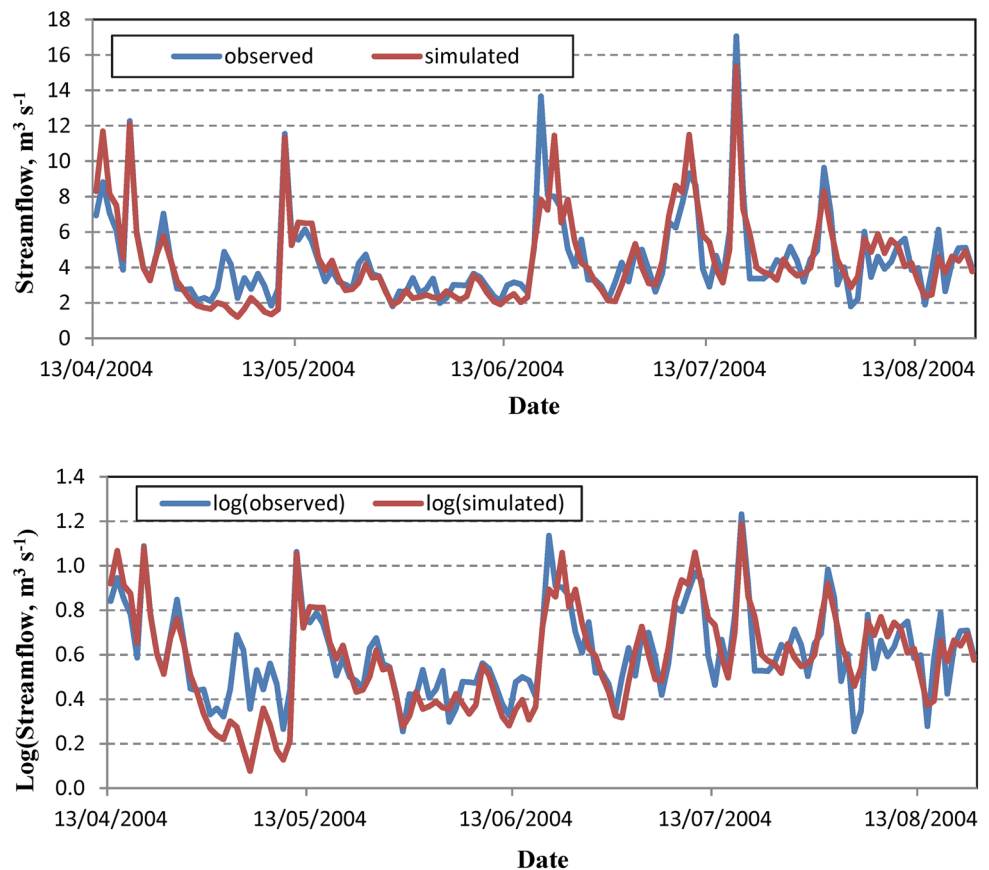


Fig. 4 Daily time-series plots for actual and log values of the observed and simulated streamflows for calibration year 2005

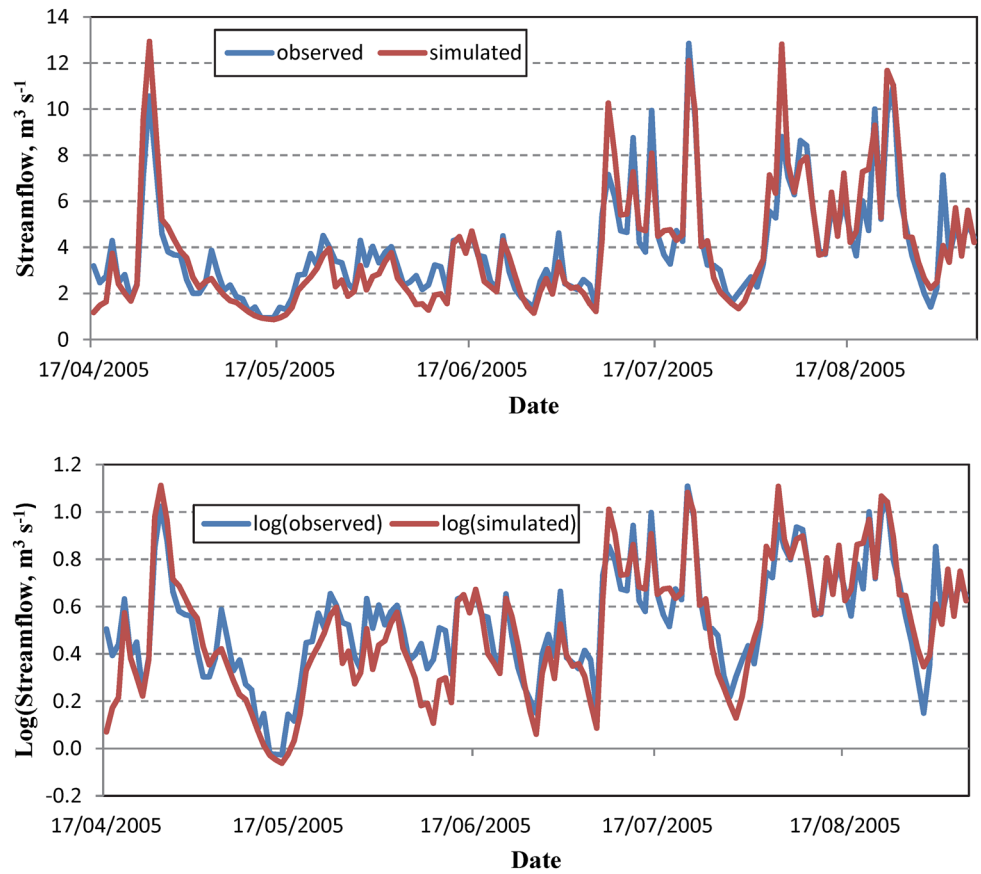


Fig. 5 Daily time-series plots for (a) actual and (b) log values of the observed and simulated streamflows for validation year 2008

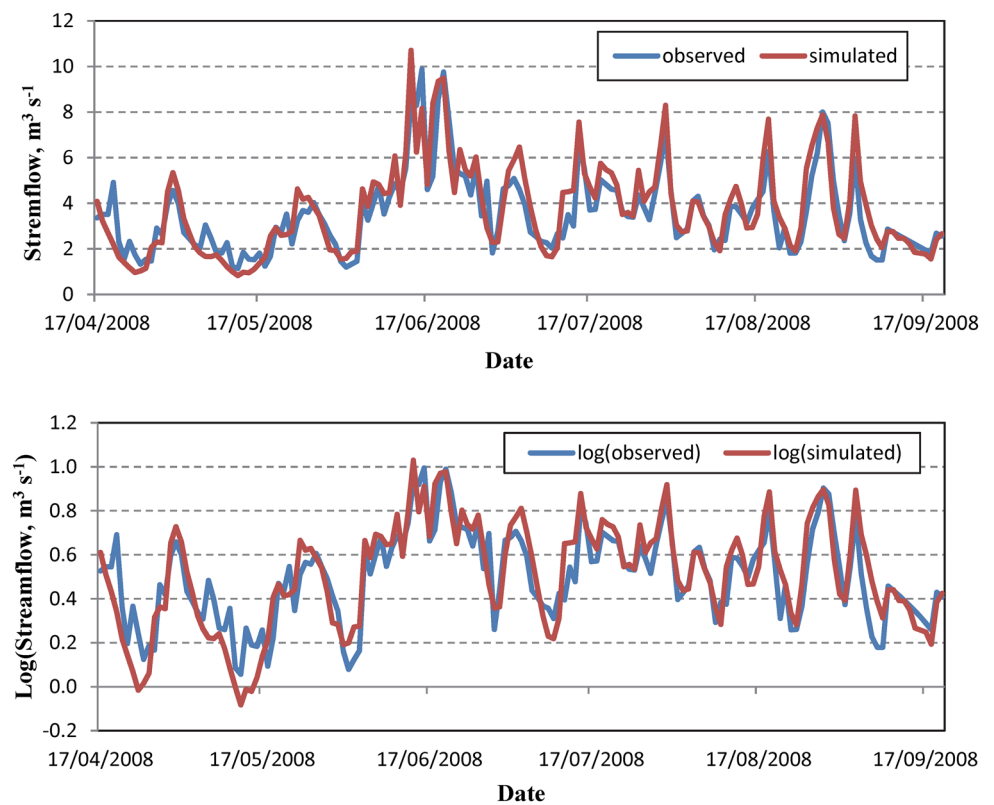
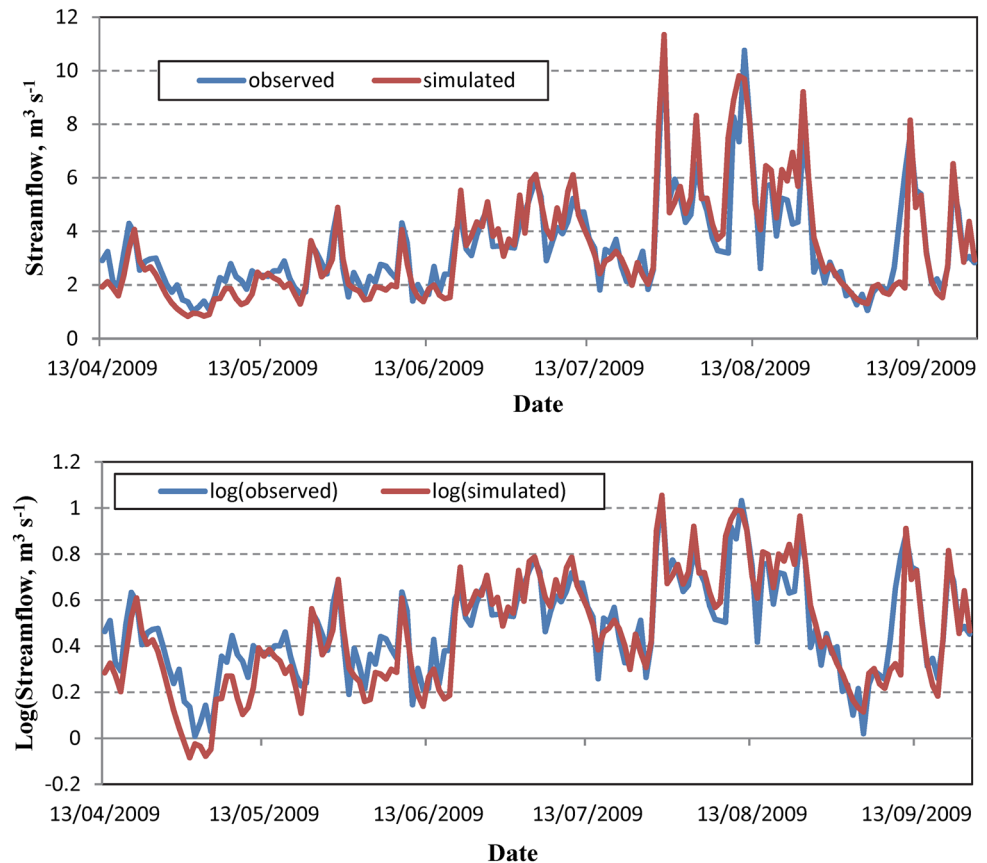


Fig. 6 Daily time-series plots for (a) actual and (b) log values of the observed and simulated streamflows for validation year 2009



1998). Changes in these values after each simulation were analyzed and percent changes in their values as compared to the previous run were calculated. Soil and plant C and N were considered to have stabilized when soil and plant C and N reached a steady/stable state, i.e., not fluctuating more than 5% for the last 10–15 years. Variation in plant C, plant N, soil C, and soil N after each spin-up year followed the same pattern for all the 4 years. Plant C stabilized after 75 years of spin-up run, while other parameters, e.g., plant N, soil C, and soil N, took less number of runs for stabilization. Therefore, 75 years of spin-up was found sufficient to stabilize plant C, plant N, soil C, and soil N.

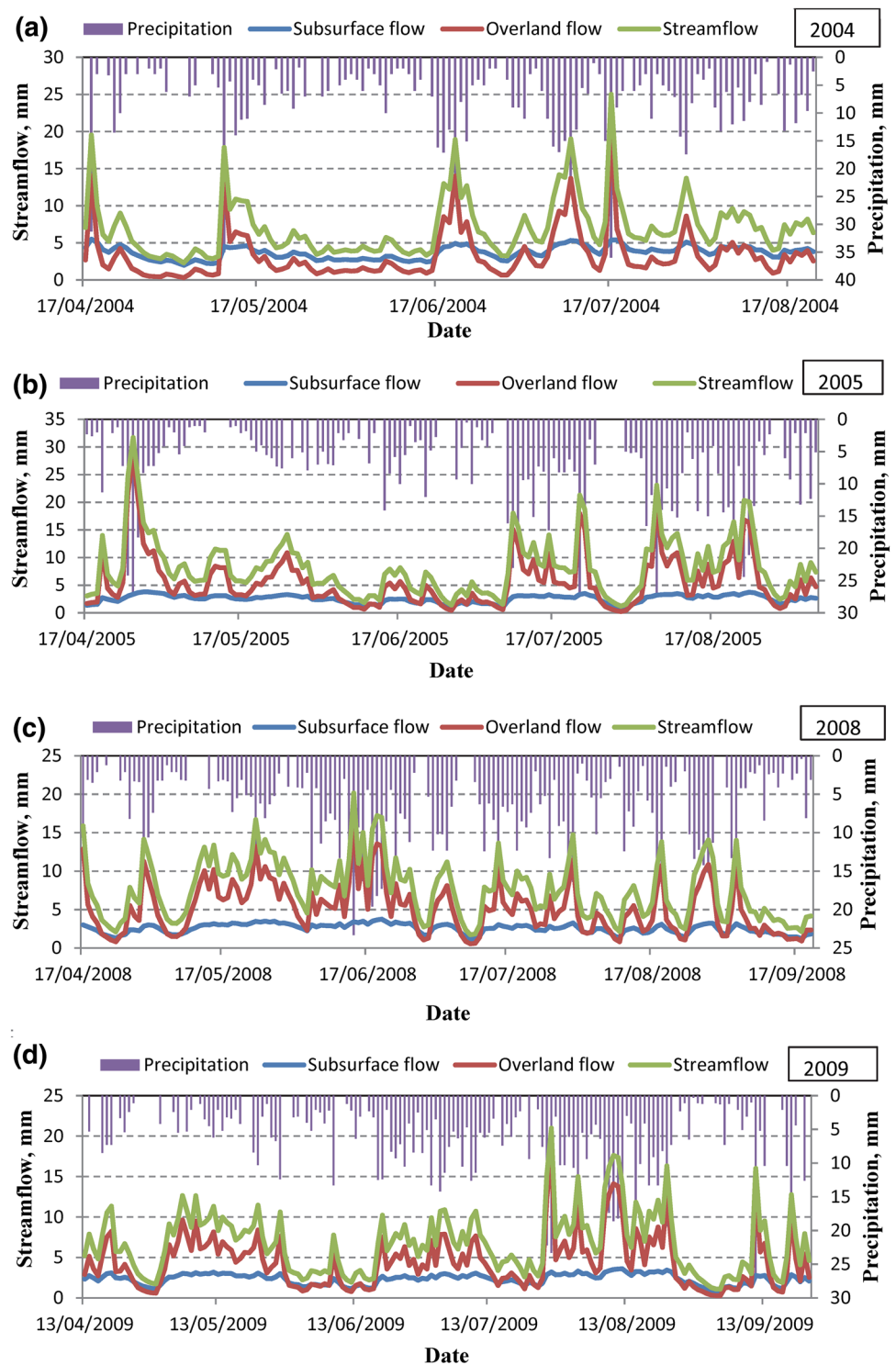
Model calibration and validation

Calibration of RHESSys was focused mainly on streamflow. The selected simulation periods were taken as 13-04-2004 to 21-08-2004 (for 2004) and 17-04-2005 to 06-09-2005 (for 2005). The best set of calibration parameters was identified by comparing simulated and observed streamflow. Calibrated parameters obtained for both the years are shown in Table 2. Figures 3 and 4 show the daily time-series plots for actual and log values of the observed and simulated streamflows for calibration years 2004 and 2005. Comparison plot of the observed and model-generated discharges showed that the observed daily discharge variations were captured well by the model. Magnitude, evolution, and variation of streamflow were well reproduced in both the calibration years. The corresponding log plots represent how well the subsurface flows are predicted by the model. Performance indicators for the calibrated simulations are presented in Table 4. The RHESSys simulated streamflow matched daily-observed discharge well with model efficiency (ME) of 0.75 and 0.82 for years 2004 and 2005, respectively. The coefficient of residual mass (CRM) was estimated to be 0.022 and 0.006 for the years 2004 and 2005, respectively, indicating negligible under-estimation. The best set of calibration parameters obtained for the two years (2004 and 2005) were averaged

Table 3 Model performance for validation years

SI No	Performance indicator	Actual streamflow		Log of streamflow	
		2008	2009	2008	2009
1	ME	0.742	0.771	0.699	0.728
2	CRM	-0.055	0.002	-0.018	0.047
3	R^2	0.811	0.834	0.783	0.824
4	SEE	0.880	0.838	0.112	0.109

Fig. 7 Time-series plots of subsurface flow, overland flow, and streamflow



to find the representative calibration parameters for the Nuranang watershed.

The calibrated model parameters were next validated using the model-simulated streamflow for years 2008 and 2009. The snow depletion period (April–September) of years 2008 and 2009 was taken as the simulation period and the

specific date ranges were 17-04-2008 to 20-09-2008 and 13-04-2005 to 23-09-2009, respectively. Simulated streamflow obtained for the validation (2008 and 2009) years were compared with the observed streamflow at the outlet of the basin. Four dimensionless statistical performance criteria, viz., ME, CRM, R^2 , and SEE, were used for validation also.

Table 4 Monthly total subsurface flow, overland flow, and total streamflow for different simulation years

Month	Streamflow component	2004		2005		2008		2009		Average	
		mm	%	mm	%	mm	%	mm	%	mm	%
April (\approx 15 days)	Subsurface flow	53.88	57.33	37.73	21.51	30.01	33.61	38.52	40.15	40.04	38.15
	Overland flow	40.10	42.67	137.69	78.49	59.28	66.40	57.43	59.85	73.63	61.85
	Total streamflow	93.99		175.42		89.28		95.95		113.66	
May (Full)	Subsurface flow	98.54	56.79	90.02	33.76	88.91	29.85	83.31	32.48	90.20	38.22
	Overland flow	74.99	43.21	176.63	66.24	208.98	70.15	173.17	67.52	158.44	61.78
	Total streamflow	173.53		266.65		297.90		256.48		248.64	
June (Full)	Subsurface flow	97.98	53.12	57.61	42.77	88.79	31.19	57.97	38.94	75.59	41.50
	Overland flow	86.48	46.89	77.08	57.23	195.86	68.81	90.89	61.06	112.58	58.50
	Total streamflow	184.45		134.69		284.65		148.86		188.16	
July (Full)	Subsurface flow	133.88	47.21	73.81	30.96	78.50	33.69	75.73	33.68	90.48	36.39
	Overland flow	149.70	52.79	164.61	69.04	154.52	66.31	149.14	66.32	154.49	63.61
	Total streamflow	283.59		238.41		233.02		224.87		244.97	
August (Full)	Subsurface flow	83.74	56.72	89.78	28.63	72.36	35.34	86.21	31.23	83.02	37.98
	Overland flow	63.90	43.28	223.78	71.37	132.42	64.66	189.83	68.77	152.48	62.02
	Total streamflow	147.64		313.56		204.78		276.04		235.51	
September (\approx 15 days)	Subsurface flow			15.22	36.79	39.74	42.08	41.31	36.66	32.09	38.51
	Overland flow			26.15	63.21	54.68	57.91	71.38	63.34	50.74	61.49
	Total streamflow			41.37		94.43		112.69		82.83	
Average	Subsurface flow									68.57	38.46
	Overland flow									117.06	61.54
	Total streamflow									185.63	

Figures 5 and 6 show the daily time-series plots for actual and log values of the observed and simulated streamflows for validation years 2008 and 2009. Comparison of the observed and model-generated discharges showed that the observed discharge variations were captured up to satisfaction in both the validation years by the model. Simulated streamflow showed a high level of agreement against observed streamflow with ME of 0.74 and 0.77 for the years 2008 and 2009, respectively (Table 3). In case of log values, the ME was obtained as 0.69 and 0.72 for 2008 and 2009, respectively, which meant that the subsurface flow in the watershed was also estimated efficiently. The corresponding CRM values obtained were -0.055 and 0.002 , respectively, indicating slight over-estimation in 2008 and slight under-estimation in 2009. Thus, the model was able to capture the hydrologic response of the watershed and simulate the water yield satisfactorily, representing the variability in streamflows.

Temporal variations in outputs of RHESSys

Daily time-series outputs of total streamflow, subsurface flow, overland flow, saturation deficit, and percent saturated

area for the watershed was generated in the model using TOPMODEL (Beven and Kirkby 1979). All these variables were obtained using the best set of calibrated parameters.

Total streamflow

Figure 7(a through d) shows daily time-series of subsurface flow, overland flow, and total streamflow at the watershed outlet during the simulation periods of year 2004, 2005, 2008, and 2009, along with daily precipitation. Total streamflow and overland flow varied directly with precipitation for all the months during simulation years, whereas assimilated daily subsurface flow remained almost constant. Daily subsurface flow and overland flow adds up to the total streamflow at the outlet. Strong seasonal variations in streamflow were observed during the simulation periods of all 4 years. In the depletion period (April–September) of all the 4 simulation years, considering the average, maximum total streamflow was observed in the month of May (248.64 mm) and minimum was observed in the month of September (82.83 mm) (Table 4). Monthly total subsurface flow was maximum in

Fig. 8 Time-series plot of saturation deficit

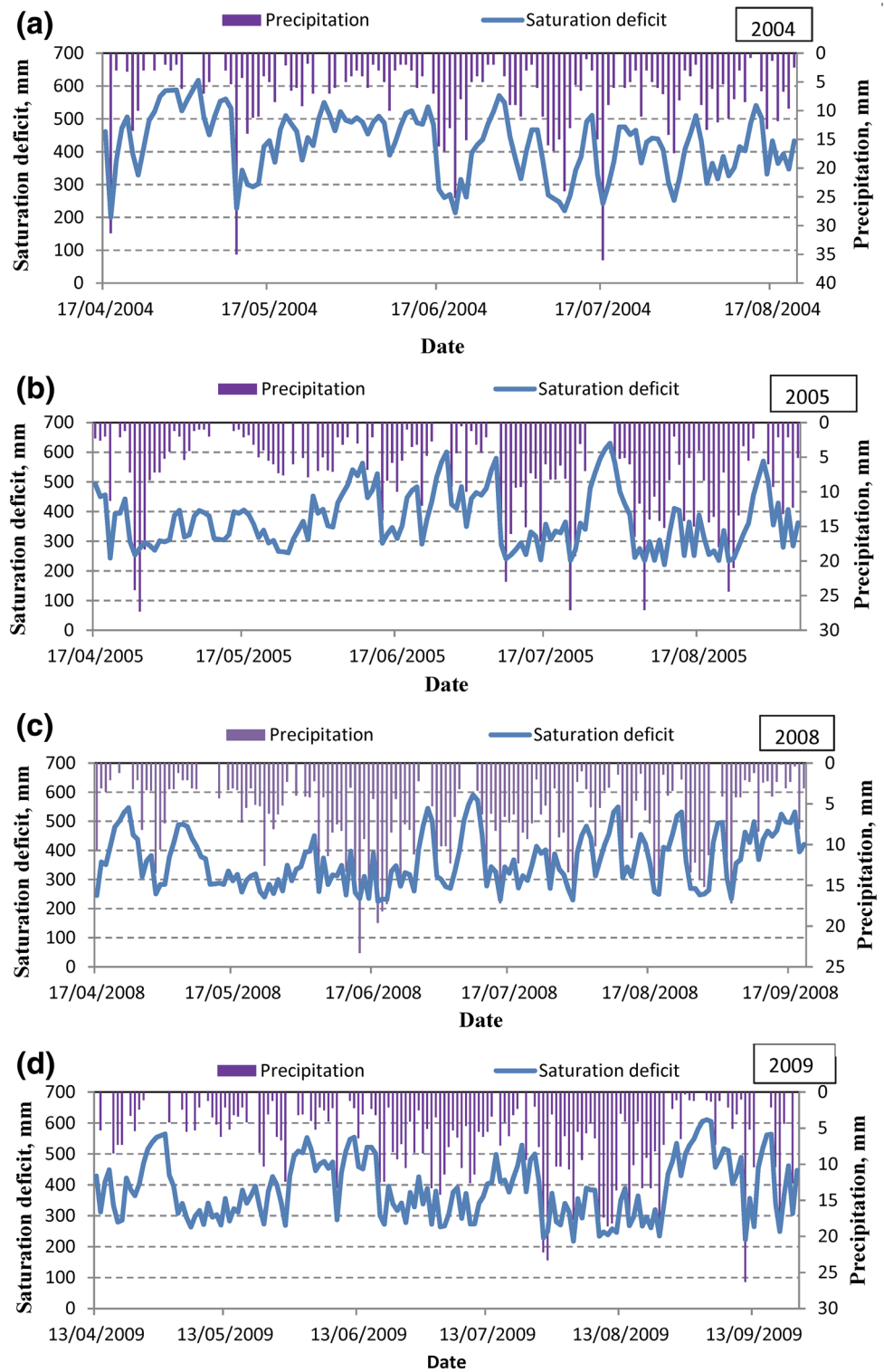


Table 5 Monthly average saturation deficit for different simulation years

Month	Saturation deficit, mm				Average
	2004	2005	2008	2009	
April	463.69	346.71	402.13	428.01	410.14
May	460.89	341.72	331.41	348.73	370.69
June	439.65	435.89	334.11	418.24	406.97
July	369.91	389.96	355.28	365.53	370.17
August	404.88	334.87	383.83	353.82	369.35
September		352.70	434.74	444.97	410.80
Overall average					389.69

the month of July (90.48 mm) and minimum in September (32.09 mm), whereas total overland flow was maximum in May (158.4 mm) and minimum in September (50.74 mm). Considering the average of all 4 simulation years, overland flow dominated stream discharge in all the months, and contributed around 60% of the total streamflow, whereas subsurface flow contributed around 40% in all the months of all simulation years. Average monthly streamflow was minimum in April, increased in May, reduced again in June, and peaked in July–August after which it subsided during September following the inverse pattern of precipitation.

Saturation deficit

Saturation deficit of soil is an index characterized by the difference between the saturation moisture content and the actual moisture content. Figure 8 (a through d) shows the daily variation in saturation deficit (mm) for the simulation years along with daily variation in observed precipitation (mm). Table 5 shows the monthly average saturation deficit (mm) for different simulation years. Analysis was restricted in the depletion period (April–September) of the simulation years only. It can be seen from Fig. 8 that the saturation deficit varied inversely with the precipitation in all the years. Considering the average of all simulation years, saturation deficit was higher in the month of April (410.14 mm) due to less precipitation in the month and was reduced in the month of May (370.69 mm), because of pre-monsoon rainfall, and increased again in June (406.97 mm) as the precipitation in June was less as compared to May. Then, it decreased again in the subsequent months of July (370.17 mm) and August (369.35 mm) due to high rainfall in monsoon season and increased again in September (410.80 mm). Considering the average of depletion period of all the simulation years, average saturation deficit was estimated as 389.69 mm.

Percentage saturated area

Percentage saturated area is the percentage of total watershed area which is under saturated condition. RHESSys provides daily output of percent saturated area ($\text{m}^2 \text{m}^{-2}$). Figure 9 (a through d) shows the daily variation in percentage saturated area along with daily precipitation in the watershed during the simulation period of 2004, 2005, 2008, and 2009, respectively. Percentage saturated area in the watershed varied directly with precipitation.

Table 6 shows the monthly average saturated area percentage corresponding to each month of different simulation years. Considering the average of all four simulation years, percentage saturated area was observed to be minimum in the month of April ($8.71 \text{ m}^2 \text{m}^{-2}$) due to low precipitation and increased in the month of May ($10.45 \text{ m}^2 \text{m}^{-2}$) due to pre-monsoon precipitation and decreased again in June ($8.63 \text{ m}^2 \text{m}^{-2}$) due to less precipitation in June as compared to May. Percentage saturated area increased again in the month of July and August ($10.35 \text{ m}^2 \text{m}^{-2}$) due to high precipitation in monsoon season, and it decreased again in September ($8.63 \text{ m}^2 \text{m}^{-2}$). Considering the average of all the simulation months, the average percentage saturated area was estimated as $9.52 \text{ m}^2 \text{m}^{-2}$.

Spatial assessment of saturation deficit

Daily spatial outputs of saturation deficit for both calibration (2004 and 2005) and validation (2008 and 2009) years were analyzed. Daily values of each pixel were averaged using ArcMap to obtain average saturation deficit map for each month. Saturation deficit was found to be minimum near streamline in low elevation areas and on stream. The number of saturated pixels increased during monsoon months and number of pixels with low saturation deficit also increased.

Figure 10 shows the spatial variation of average monthly saturation deficit in the Nuranang watershed for April–August 2004. Strong spatial variation in saturation deficit was observed during the simulation period. The average saturation deficit varied from 0 to 911.63 mm during the simulation period of 2004. Average saturation deficit was minimum in July and maximum in April and varied inversely with precipitation. The number of pixels with minimum (0–100 mm) saturation deficit was minimum in May and maximum in July. During the simulation period of 2005 (Fig. 11), average saturation deficit varied from 0 to 900.03 mm with a high value during April–May, which reduced later during June–August, but reached maximum in September indicating an opposite trend with precipitation.

Fig. 9 Time-series output of percentage saturated area

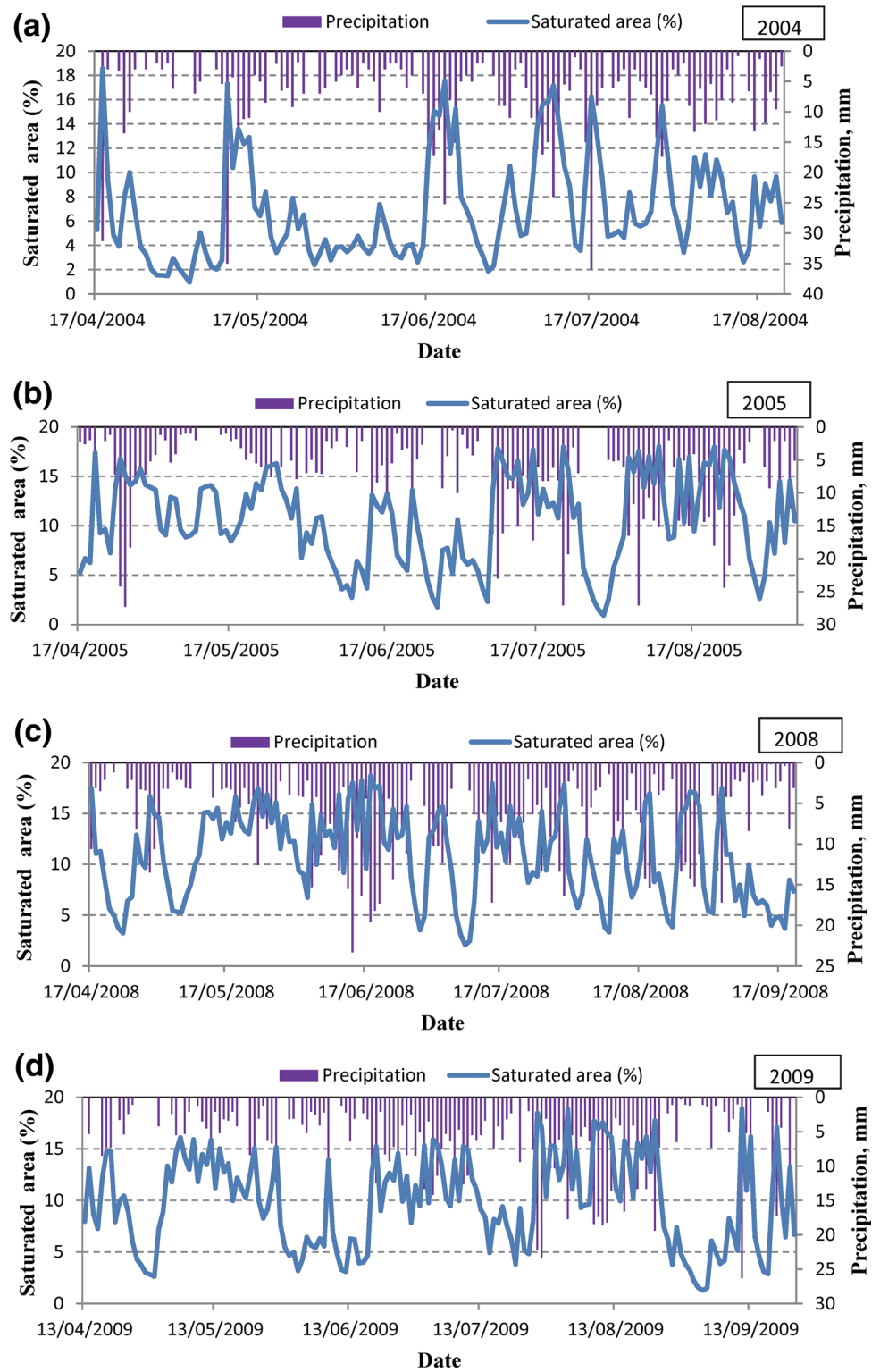


Table 6 Monthly average percentage saturated area for different simulation years

Month	Percentage saturated area ($\text{m}^2 \text{m}^{-2}$)				Average
	2004	2005	2008	2009	
April	5.74	11.85	9.17	8.08	8.71
May	5.55	11.93	12.59	11.74	10.45
June	6.28	7.47	12.48	8.27	8.63
July	9.22	10.09	11.35	10.73	10.35
August	7.35	12.44	9.97	11.62	10.35
September		10.88	7.56	7.46	8.63
Overall average					9.52

The number of pixels with minimum saturation deficit was minimum in May and maximum in August and September. For 2008 (Fig. 12), monthly average saturation deficit varied from 0 to 764.98 mm over all pixels during the simulation period of 2008. Monthly average saturation deficit was high in April, reduced in May–June, and then increased again in July–August. The number of pixels with low saturation deficit was minimum in the month of April and maximum in the month of June. In 2009, monthly average saturation deficit varied from 0 to 903.70 mm over the watershed's spatial extent (Fig. 13). Spatial distribution of saturation deficit showed that a number of pixels with low saturation deficit were minimum in April and May, whereas the number of saturated pixels was maximum in monsoon month of July and August. Considering the average of all four-simulation years, a number of saturated pixels were minimum in April–May and maximum in August.

Summary and conclusions

RHESSys model is one of the best models for estimating spatial assessment of saturation deficit in a mountainous watershed where both hydrological and ecological variables have great impact on watershed hydrology. The model was simulated, calibrated, and validated successfully for the Nuranang watershed in the Eastern Himalayan region. Calibration of the model was done successfully for the years 2004 and 2005 using observed streamflow at watershed outlet. Average calibrated values of four calibration parameters (multiplier to the value provided in default file): decay of hydraulic conductivity with depth (m) and soil hydraulic conductivity at surface (K); and two groundwater parameters ($gw1$ and $gw2$) were obtained as 0.1475, 40.3386, 0.2391, and 0.1983, respectively. The calibrated model parameters were validated using the

model-simulated streamflow for years 2008 and 2009. Simulated streamflows showed a high level of agreement against observed streamflow with ME of 0.74 and 0.77 for the years 2008 and 2009, respectively. For all the simulation years, total streamflow and overland flow followed the same pattern, whereas subsurface flow remained almost constant. Strong seasonal variations in total streamflow were observed during the simulation periods for all 4 years. The pattern of streamflow and overland flow and overland flow followed the same trend as total precipitation in all simulation years. Considering the average of all four-simulation years, maximum total streamflow was observed in the month of May (248.64 mm). Considering average of all the simulation years, overland flow contributed around 60% of total streamflow, and subsurface flow contributed around 40%. Saturation deficit was varying inversely with the precipitation. Maximum saturation deficit was observed in April as the rainfall was low in the month and it decreased in May due to pre-monsoon rainfall received. Average saturation deficit again increased in June as June month received less rainfall as compared to May, and it decreased again in July and August being the peak monsoon months and increased again in September. Considering average of all the simulation months, average saturation deficit was estimated as 389.69 mm. Percentage saturated area in the watershed varied directly with precipitation. Average percentage saturated area was observed to be minimum in the month of April, and increased in the month of May. It decreased in June and increased in July and August and then decreased again in September. Considering average of all the simulation months, average percentage saturated area was estimated as 9.52 $\text{m}^2 \text{m}^{-2}$. Spatial variation of saturation deficit showed that saturation deficit was low in low elevation region near streamline for all the months in all simulation years. The number of pixels with low saturation deficit was less in April–May. During monsoon season, the number of saturated pixels increased and number of pixels with low saturation deficit also increased. It can be concluded that total streamflow, overland flow, and saturation deficit in the watershed are directly influenced by precipitation. Streamflow and overland flow varied directly with precipitation, whereas saturation deficit varied inversely with precipitation. The calibrated model can be used to simulate the effects of climate and land-use/land-cover change on streamflow and other hydrologic variables.

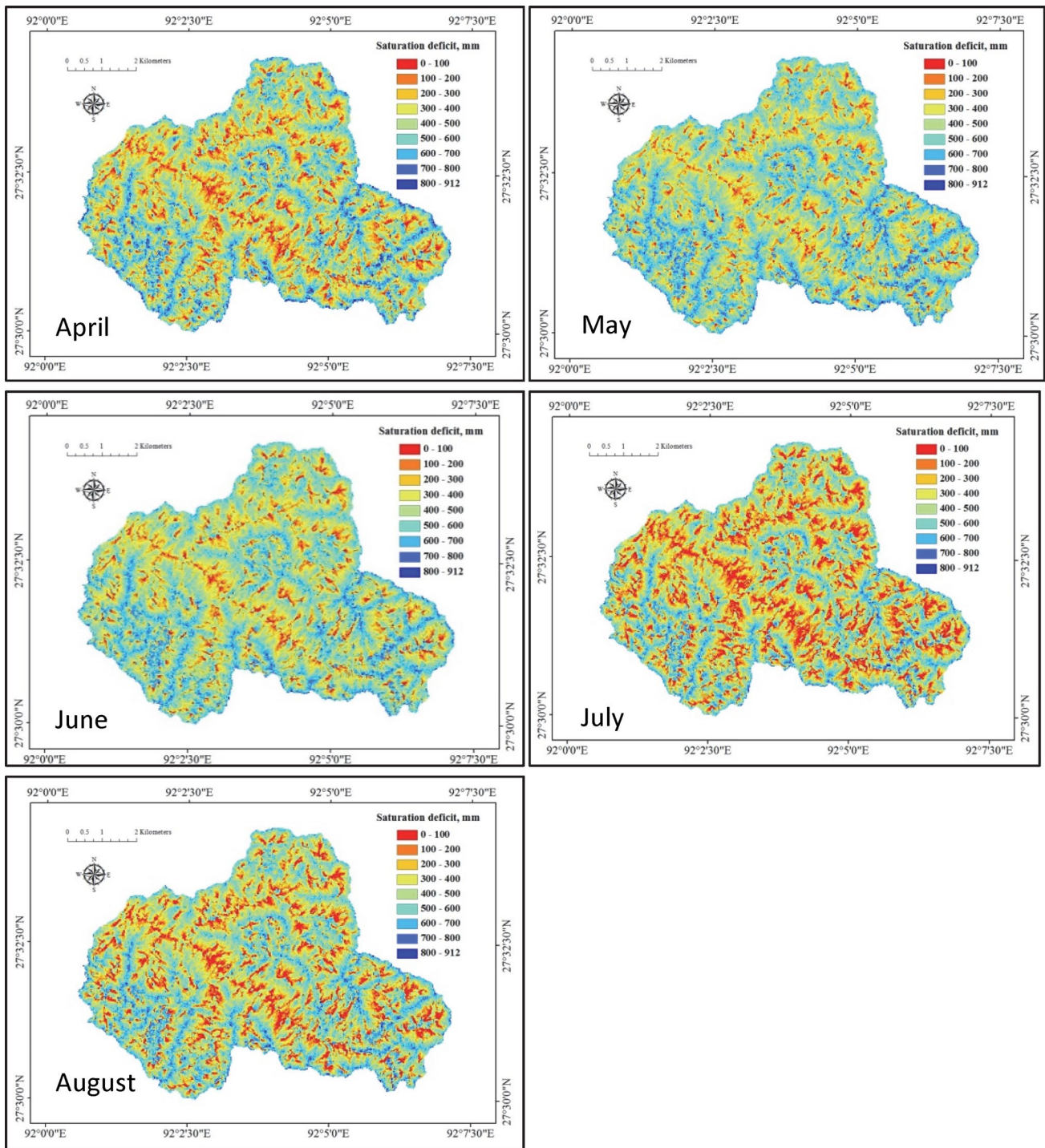


Fig. 10 Monthly average saturation deficit for each month in 2004

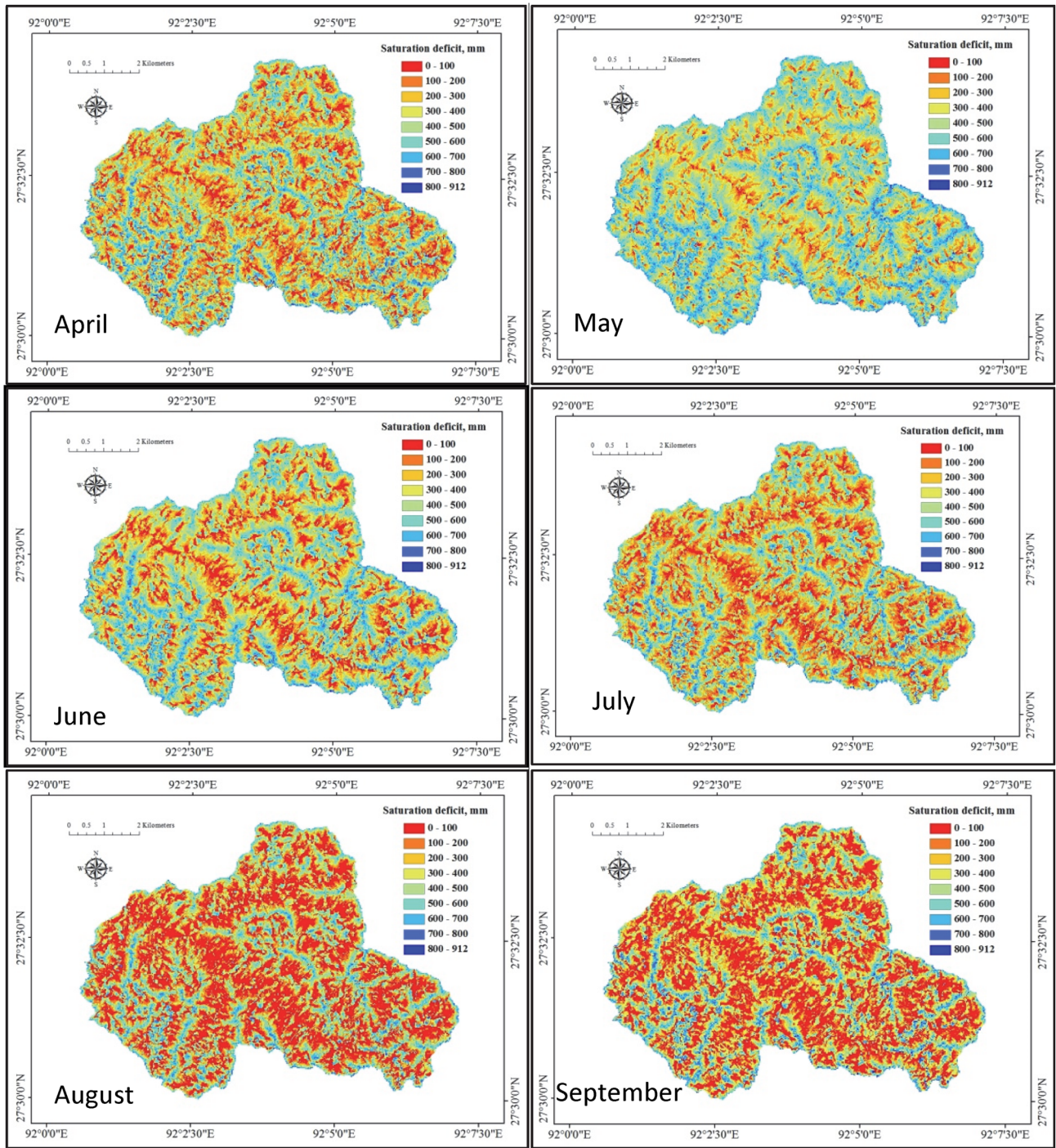


Fig. 11 Monthly average saturation deficit for each month in 2005

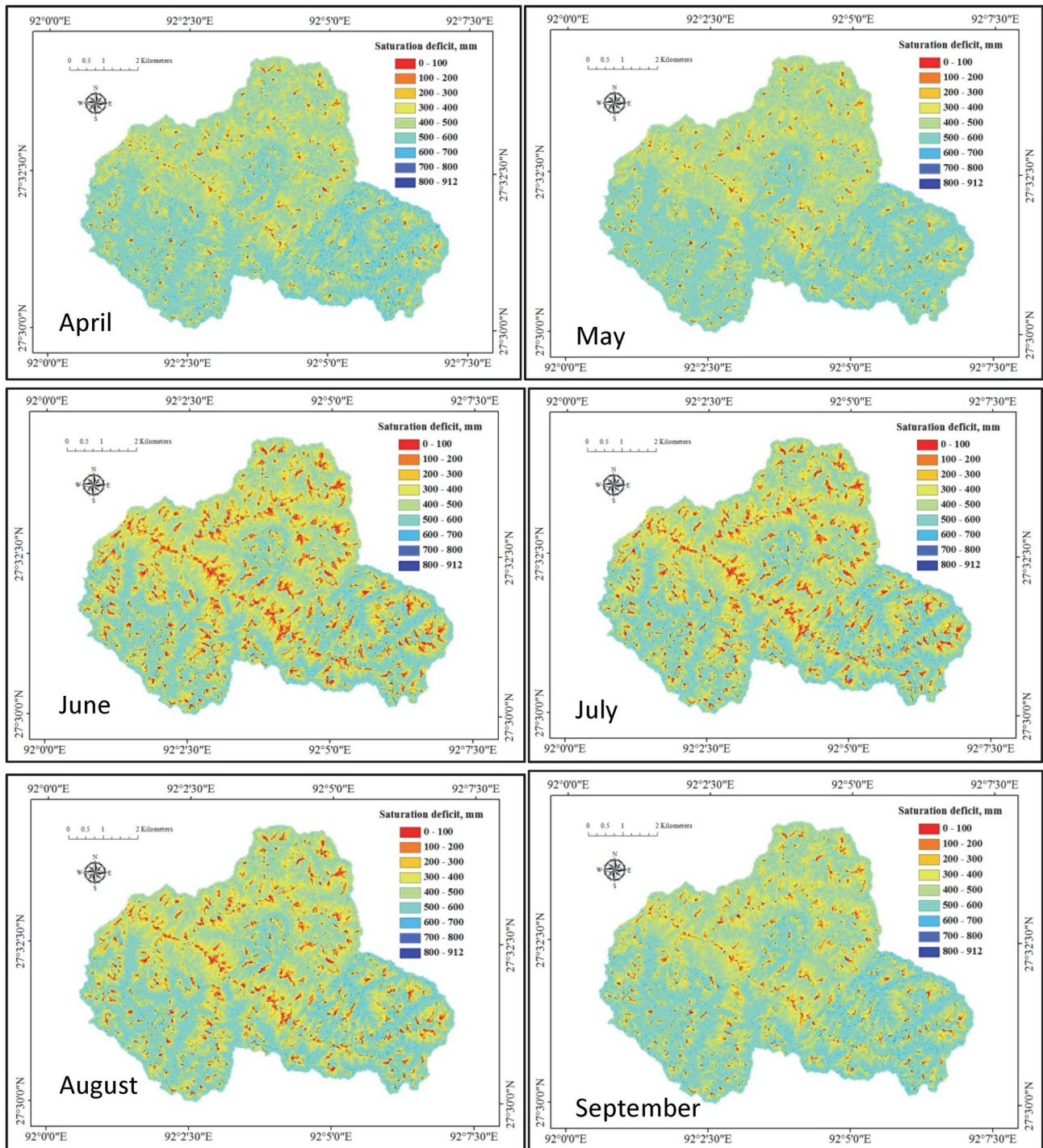


Fig. 12 Monthly average saturation deficit for each month in 2008

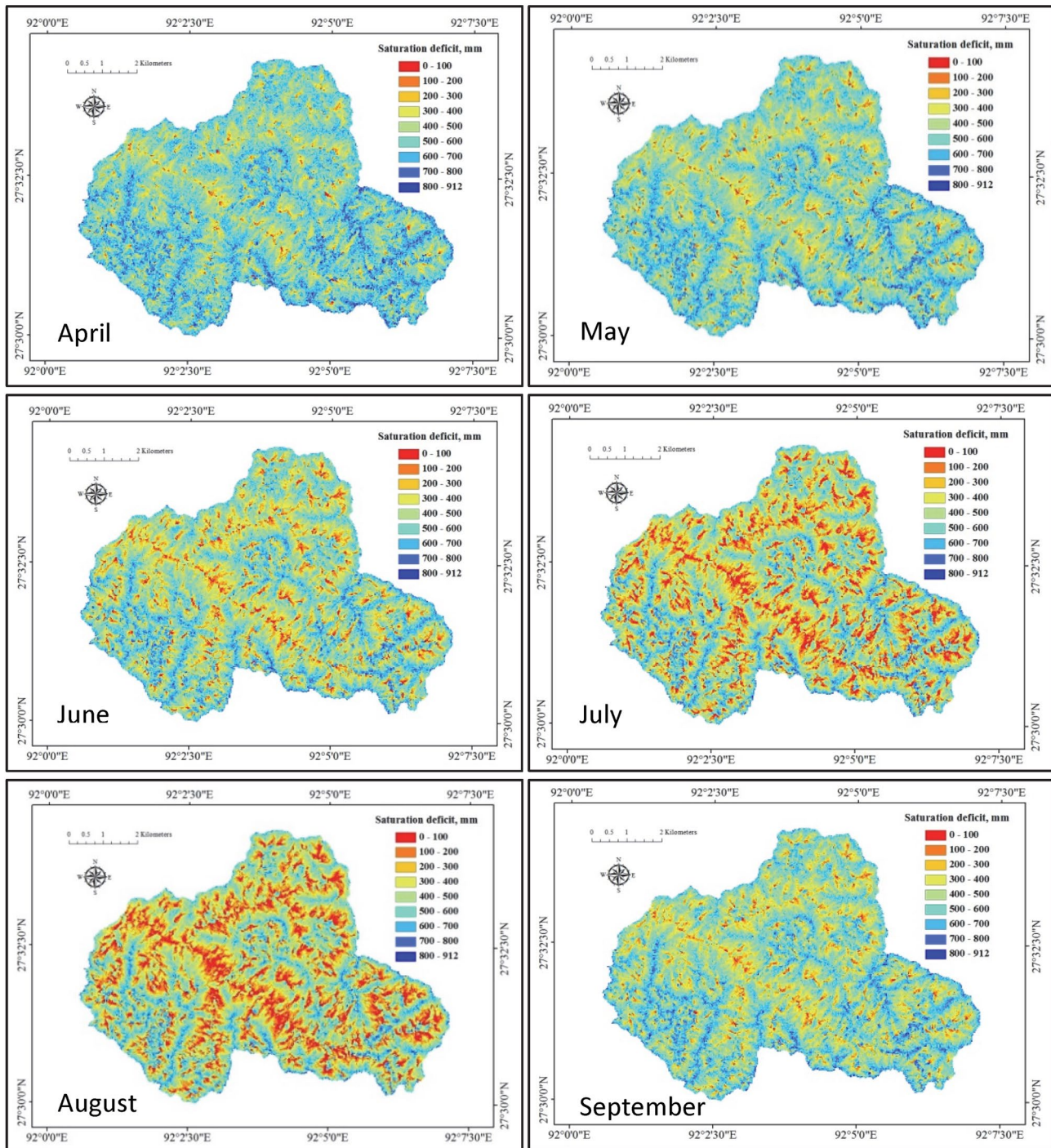


Fig. 13 Monthly average saturation deficit for each month in 2009

References

Aawar T, Khare D (2020) Assessment of climate change impacts on streamflow through hydrological model using SWAT model: a case study of Afghanistan. *Model Earth Syst Environ* 6:1427–1437

Allen SE, Grimshaw HM, Parkinson JA, Quarmby C (1974) *Chemical analysis of ecological materials*. Blackwell Scientific Publication, London

Band LE, Patterson P, Nemani R, Running SW (1993) Forest ecosystem processes at the watershed scale: incorporating hillslope hydrology. *Agr Forest Meteorol* 63:93–126

- Band LE, Mackay DS, Creed IF (1996) Ecosystem processes at the watershed scale: Sensitivity to potential climate change. *Limnol Oceanogr* 41(5):928–938
- Band LE, Tague CL, Groffman P, Belt K (2001) Forest ecosystem processes at the watershed scale: hydrological and ecological controls of nitrogen export. *Hydrol Process* 15:2013–2028
- Bandyopadhyay A, Bhadra A, Maza M, Shelina RK (2014) Monthly Variations of Air Temperature Lapse Rates in Arunachal Himalaya. *J Indian Water Resour Soc* 34 (3).
- Baron JS, Hartman MD, Kittel TGF, Band LE, Ojima DS, Lammers RB (1998) Effects of land cover, water redistribution, and temperature on ecosystem processes in the South Platte Basin. *Ecol Appl* 8:1037–1051
- Beven KJ, Kirkby MJ (1979) A physically based, variable contributing area model of basin hydrology / Un modèle à base physique de zone d'appel variable de l'hydrologie du bassin versant. *Hydrol Sci Bull* 24(1):43–69
- Bolstad PV, Swift L, Collins F, Regnier J (1998) Measured and predicted air temperatures at basin to regional scales in the southern Appalachian Mountains. *Agric For Meteorol* 91(3–4):161–176
- Boufala M, Hmaidi AE, Chadli K, Essahlaoui A, Ouali AE, Taia S (2019) Hydrological modeling of water and soil resources in the basin upstream of the Allal El Fassi dam (Upper Sebou watershed, Morocco). *Model Earth Syst Environ* 5:1163–1177
- Cahyono C, Adidarma WK (2019) Influence analysis of peak rate factor in the flood events' calibration process using HEC–HMS. *Model Earth Syst Environ* 5:1705–1722
- Chaemiso SE, Abebe A, Pingale SM (2016) Assessment of the impact of climate change on surface hydrological processes using SWAT: a case study of Omo-Gibe river basin, Ethiopia. *Model Earth Syst Environ* 2:1–15
- Chawla I, Mujumdar PP (2015) Isolating the impact of land use and climate change on streamflow. *Hydrol Earth Syst Sci* 19:3633–3651
- Eagleson P (1978) Climate, soil and vegetation. 3. A simplified model of soil moisture movement in the liquid phase. *Water Resour Res* 14:722–730
- Gorelick DE, Lin L, Zeff HB, Kim Y, Vose JM, Coulston JW, Wear DN, Band LE, Reed PM, Characklis GW (2020) Accounting for adaptive water supply management when quantifying climate and land cover change vulnerability. *Water Resour Res* 56:27
- Hartman MD, Baron J, Lammers RB, Cline DW, Band LE, Liston GE, Tague C (1999) Simulations of snow distribution and hydrology in a mountain basin. *Water Resour Res* 35(5):1587–1603
- Hosseini SH, Khaleghi MR (2020) Application of SWAT model and SWAT-CUP software in simulation and analysis of sediment uncertainty in arid and semi-arid watersheds (case study: the Zoshk-Abardeh watershed). *Model Earth Syst Environ* 6:2003–2013
- Hwang T, Kang S, Kim J, Kim Y, Lee D, Band LE (2008) Evaluating drought effect on MODIS gross primary production (GPP) with an eco-hydrological model in the mountainous forest. *East Asia Glob Chang Biol* 14(5):1037–1056
- Khatun S, Sahana M, Jain SK, Jain N (2018) Simulation of surface runoff using semi distributed hydrological model for a part of Satluj Basin: parameterization and global sensitivity analysis using SWAT CUP. *Model Earth Syst Environ* 4:1111–1124
- Kim ES, Kang SK, Lee BR, Kim KH, Kim J (2007) Parameterization and application of regional hydro-ecologic simulation system (RHESSys) for integrating the eco-hydrological processes in the Gwangneung headwater catchment. *Korean J Agric For Meteorol* 9(2):121–131
- Le Bissonnais Y, Daroussin J, Jamagne M, Lambert JJ, Le Bas C, King D, Cerdan O, Leonard J, Bresson LM, Jones RJA (2005) Pan-European soil crusting and erodibility assessment from the European soil geographical database using pedotransfer rules. *Adv Environ Monitor Modell* 12:1–15
- Mandal SP, Chakrabarty A (2016) Flash flood risk assessment for upper Teesta river basin: using the hydrological modeling system (HEC-HMS) software. *Model Earth Syst Environ* 2:59
- Mengistu SG, Ali MA, Yassin FA (2016) Assessment of the sensitivity of streamflow simulations to change in patch resolution using GIS based hydro-ecological model. *Open J Modern Hydrol* 6:66–78
- Meresa H (2019) Modelling of river flow in ungauged catchment using remote sensing data: application of the empirical (SCS-CN), Artificial Neural Network (ANN) and Hydrological Model (HEC-HMS). *Model Earth Syst Environ* 5:257–273
- Mishra V, Lilhare R (2016) Hydrologic sensitivity of Indian sub-continental river basins to climate change. *Glob Planet Change* 139:78–96
- Mohammed IN, Tarboton DG (2014) Simulated watershed responses to land cover changes using the regional hydro-ecological simulation system. *Hydrol Process* 28(15):4511–4528
- Monteith J (1965) Evaporation and the environment. In: *Proceedings of the 19th symposium of the society for experimental biology*. Cambridge University Press, 205–233
- Moran-Tejada E, Zabalza J, Rehman K, Gago-Silva A, Lopez-Moreno JJ, Vicente-Serrano S, Lehmann A, Tague CL, Beniston M (2015) Hydrological impacts of climate and land-use changes in a mountain watershed: Uncertainty estimation based on model comparison. *Ecohydrol* 8:1396–1416
- Natrajan S, Radhakrishnan N (2019) Simulation of extreme event-based rainfall–runoff process of an urban catchment area using HEC-HMS. *Model Earth Syst Environ* 5:1867–1881
- Patil NS, Nararaja M (2020) Effect of land use land cover changes on runoff using hydrological model: a case study in Hiranyakeshi watershed. *Model Earth Syst Environ* 6:2345–2357
- Paul M, Negahban-Azar M (2018) Sensitivity and uncertainty analysis for streamflow prediction using multiple optimization algorithms and objective functions: San Joaquin Watershed, California. *Model Earth Syst Environ* 4:1509–1525
- Phillip J (1957) The theory of infiltration: 4. Sorptivity and algebraic infiltration equation. *Soil Sci* 84:257–264
- Praveen KBJ, Pradeep H, Lokesh A, Akarshraj KH, Surendra HJ, Avinash HD (2016) Estimation of runoff using empirical equations and fuzzy logic method: a case study. *Int J Sci Eng Res* 7(5)
- Prihodko L, Goward SN (1997) Estimation of air temperature from remotely sensed surface observations. *Remote Sens Environ* 60(3):335–346
- Sanford SE, Creed IF, Tague CL, Beall FD, Buttle JM (2007) Scale-dependence of natural variability of flow regimes in a forested landscape. *Water Resour Res* 43:W08414
- Schwab GO, Fangmeier DD, Elliot WJ, Frevert RK (1993) *Soil and water conservation engineering*, 4th edn. John Wiley & Sons Inc, New York
- Shah HL, Mishra V (2016) Hydrologic changes in Indian subcontinental river basins (1901–2012). *J Hydrometeorol* 17:2667–2687
- Shin H, Park M, Lee J, Lim H, Kim SJ (2019a) Evaluation of the effects of climate change on forest watershed hydroecology using the RHESSys model: Seolmacheon catchment. *Paddy Water Environ* 17:581–595
- Shin H, Park M, Lee J, Lim H, Kim SJ (2019b) Evaluation of the effects of climate change on forest watershed hydroecology using the RHESSys model: Seolmacheon catchment. *Paddy Water Environ* 17:581–595
- Srivastava PC (2000) *Soils of Arunachal Pradesh*. SLUB Publ. 18, State Land Use Board, Naharlagun-791110 86+ one sheet of soil map.
- Tague CL, Band LE (2001) Evaluating explicit and implicit routing for watershed hydro-ecological models of forest hydrology at the small catchment scale. *Hydrol Process* 15:1415–1439
- Tague CL, Band LE (2004) RHESSys: regional hydro-ecologic simulation system—an object-oriented approach to spatially distributed

- modeling of carbon, water, and nutrient cycling. *Earth Interact* 8(19):1–42
- Tague C, Peng H (2013) The sensitivity of forest water use to the timing of precipitation and snowmelt recharge in the California Sierra: implications for a warming climate. *J Geophys Res* 118(2):875–887
- Thornton P (1998) Regional ecosystem simulation: Combining surface and satellite based observations to study linkages between terrestrial energy and mass budgets. Ph.D. thesis, School of Forestry, University of Montana, Missoula.
- Tsamir M, Gottlieb S, Preisler Y, Rotenberg E., Tatarinov F, Yakir D, Tague C, Klein T (2019) Stand density effects on carbon and water fluxes in a semi-arid forest, from leaf to stand-scale. *For. Ecol. Manag.* 453(117573)
- Wigmosta MS, Vail LW, Lettenmaier DP (1994) A distributed hydrology-vegetation model for complex terrain. *Water Resour Res* 30(6):1665–1679
- Wolock DM (1993) Simulating the variable-source-area concept of streamflow generation with the watershed model Topmodel. U.S. Geological Survey Water-Resources Investigations Report 93–4124

Publisher's Note Springer Nature remains neutral with regard to jurisdictional claims in published maps and institutional affiliations.